Earth and Planetary Science Letters 285 (2009) 355–363

Contents lists available at ScienceDirect

Earth and Planetary Science Letters

journal homepage: www.elsevier.com/locate/epsl

Shallow basins on Mercury: Evidence of relaxation?

P. Surdas Mohit [a,b,*], Catherine L. Johnson [a,b], Olivier Barnouin-Jha [c], Maria T. Zuber [d], Sean C. Solomon [e]

[a] Department of Earth and Ocean Sciences, University of British Columbia, Vancouver, BC, Canada V6T 1Z4
[b] Institute of Geophysics and Planetary Physics, Scripps Institution of Oceanography, La Jolla, CA 92093, USA
[c] The Johns Hopkins University Applied Physics Laboratory, Laurel, MD 20723, USA
[d] Department of Earth, Atmospheric, and Planetary Sciences, Massachussetts Institute of Technology, Cambridge, MA 02139, USA
[e] Department of Terrestrial Magnetism, Carnegie Institution of Washington, Washington, DC 20015, USA

ARTICLE INFO

Article history:
Accepted 15 April 2009
Available online 28 May 2009

Editor: T. Spohn

Keywords:
Mercury
MESSENGER
Caloris
impact basins
viscous relaxation

ABSTRACT

Stereo-derived topographic models have shown that the impact basins Beethoven and Tolstoj on Mercury are shallow for their size, with depths of 2.5 and 2 (±0.7) km, respectively, while Caloris basin has been estimated to be 9 (±3) km deep on the basis of photoclinometric measurements. We evaluate the depths of Beethoven and Tolstoj in the context of comparable basins on other planets and smaller craters on Mercury, using data from Mariner 10 and the first flyby of the MESSENGER spacecraft. We consider three scenarios that might explain the anomalous depths of these basins: (1) volcanic infilling, (2) complete crustal excavation, and (3) viscoelastic relaxation. None of these can be ruled out, but the fill scenario would imply a thick lithosphere early in Mercury's history and the crustal-excavation scenario a pre-impact crustal thickness of 15–55 km, depending on the density of the crust, in the area of Beethoven and Tolstoj. The potential for viscous relaxation of Beethoven, Tolstoj, and Caloris is explored with a viscoelastic model. Results show that relaxation of these basins could occur at plausible heat flux values for a range of crustal thicknesses. However, the amplitude of current topographic relief points to a crustal thickness of at least 60 km under this hypothesis. Relaxation of Caloris may have occurred if the floor is underlain by crust at least 20 km thick. We discuss future observations by MESSENGER that should distinguish among these scenarios.

1. Introduction

The mechanism responsible for Mercury's high bulk density and implied high bulk iron content remains a mystery, although three classes of models have been proposed: (1) metal-silicate fractionation by differential aerodynamic drag in the early solar nebula, (2) vaporization of the silicate crust and mantle in a hot solar nebula, and (3) removal of most of the crust and mantle by giant impact (Solomon, 2003; Benz et al., 2007). These hypotheses have different consequences for the current thickness and composition of Mercury's crust. While the metal-silicate fractionation hypothesis could result in a thick early crust, the latter two hypotheses would remove a large fraction of any early crust, with the result that the bulk of the present crust of Mercury would be of secondary origin (i.e., produced by partial melting of the residual mantle). Each would also have important consequences for Mercury's thermal history, because of differences in the post-accretion temperature distribution and abundances of long-lived radioactive elements. For example, high initial temperatures would produce more contraction, whereas a radioactive element budget consistent with the vaporization hypothesis would predict a smaller inner core size at present than for alternative models with otherwise similar assumptions and adopted parameter values (e.g., Hauck et al., 2004; Breuer et al., 2007). Placing constraints on the crustal thickness and thermal evolution of Mercury is therefore an important step in understanding Mercury's anomalous composition.

Previous attempts to constrain crustal thickness have been limited by available information. Anderson et al. (1996) combined equatorial topography obtained from Earth-based radar with the Mariner 10 determination of C_{22}, the degree-2 tesseral coefficient in the spherical harmonic expansion of Mercury's gravity field. Under the assumption of isostasy, they estimated a depth of compensation of 200 ± 100 km. However, this calculation tends to overestimate crustal thickness, producing depths of compensation of 80 km for the Moon and 400 km for Mars, whereas average crustal thicknesses are thought to be in the range 40–60 km (Wieczorek and Zuber, 2004; Hikida and Wieczorek, 2007) and 30–70 km (Neumann et al., 2004; Wieczorek et al., 2006), respectively.

The thermal and mechanical structure of the planet has also been inferred from geological observations. From stereo-derived topographic profiles, Watters et al. (2002) estimated the depth of faulting at Discovery Rupes — the longest-known lobate scarp at that time — to be 35–40 km. At the time of faulting, the elastic lithosphere should

* Corresponding author. Department of Earth and Ocean Sciences, University of British Columbia, Vancouver, BC, Canada V6T 1Z4.
E-mail address: smohit@eos.ubc.ca (P.S. Mohit).

0012-821X/$ – see front matter © 2009 Elsevier B.V. All rights reserved.
doi:10.1016/j.epsl.2009.04.023

have been at least as thick, implying a heat flux no greater than 40 mW m^{-2}. Models of the viscous relaxation of isostatically compensated relief predict that the crustal thickness must be less than 200 km (Nimmo, 2002) in order that the modern long-wavelength topography be preserved. Watters et al. (2005) proposed that the Caloris impact basin may have relaxed by inward flow of the lowermost crust, a scenario requiring a crustal thickness of at least 90 km beneath the basin according to their calculations.

André et al. (2005) have shown from stereogrammetric topography that the Tolstoj (15°S, 165°W) and Beethoven (20°S, 124°W) basins appear shallower than would be expected for their size, an observation potentially consistent with viscous relaxation. Here we examine the depths of these impact basins in the context of the dimensions of smaller craters, using stereo-derived topographic maps and data from the Mercury Laser Altimeter (MLA) on the MErcury Surface, Space ENvironment, GEochemistry, and Ranging (MESSENGER) spacecraft and measurements of the depths of large basins on other planets. We consider three scenarios for basin evolution, with a focus on viscous relaxation, and we explore the consequences for the Caloris basin. Finally, we consider how this issue can be resolved with data to be obtained by MESSENGER in the future.

2. Depth–diameter relations for craters and basins on Mercury

The Caloris basin, with a diameter of 1550 km, is the largest well-preserved impact basin on the planet. The interior of the basin is partially filled with smooth plains deposits, which are likely of volcanic origin (Spudis and Guest, 1988; Head et al., 2008; Murchie et al., 2008). The smooth plains have been deformed by wrinkle ridges similar to those in lunar mare basins and similarly attributable to subsidence of the basin following plains emplacement (Kennedy et al., 2008; Murchie et al., 2008).

Unlike any lunar basin, Caloris also exhibits an extensive system of extensional troughs that are younger than the wrinkle ridges and display orientations that range from radial at the center to dominantly circumferential at the edge of the basin (Murchie et al., 2008). Models for the formation of these troughs include relaxation of basin relief by lateral crustal flow (Watters et al., 2005) and uplift of the floor due to exterior loading (Melosh and McKinnon, 1988; Kennedy et al., 2008). Although the depth of the basin has not yet been accurately measured, Mariner 10 photoclinometric measurements suggest a rim-to-floor depth of 9 ± 3 km (Hapke et al., 1975).

Beethoven and Tolstoj are the only major basins on Mercury for which stereo-derived digital elevation models (DEMs) are currently available (André et al., 2005). The morphologies of the basins show that they predate Caloris, and younger smooth plains units cover the floors of each (Spudis and Guest, 1988). In contrast to Caloris, geologic maps show only a few wrinkle ridges around the edges of Tolstoj (Schaber and McCauley, 1980) and none in Beethoven (Spudis and Prosser, 1984); no extensional faults have been mapped in either basin.

Beethoven has a diameter (D) of ~600 km and an estimated rim-to-floor depth (d) of $\sim 2.5 \pm 0.7$ km, whereas $D = 440$ km and $d \sim 2 \pm 0.7$ km for Tolstoj (André et al., 2005). The estimated topographic uncertainty of the DEMs is ~0.5 km. Schenk and Bussey (2004), however, reported that stereo-derived DEMs of the Moon obtained from Galileo images showed long-wavelength (wavelength ~1500 km) misfits of around 450 m with respect to the absolute topographic measurements made by the Clementine laser rangefinder. As it is difficult to estimate the long-wavelength error in the Mercury stereogrammetry until MLA profiles coincide with areas imaged by Mariner 10 or MESSENGER, we will use 450 m as an initial estimate of that error. If the two contributions to the DEM errors are independent, the combined error in the depth estimates is ~700 m. Such a large uncertainty in depth complicates attempts to understand basin evolution.

A comparison of the depths of these basins to their counterparts on the Moon and Mars (Fig. 1A) shows that Tolstoj and Beethoven are relatively shallow. Lunar basins in a similar size range show depths of 4.1–5.5 km (Williams and Zuber, 1998), while the only well-preserved basin on Mars with $D < 1000$ km, Newton ($D = 305$ km), has a depth of ~4 km (Howenstine and Kiefer, 2005; Mohit and Phillips, 2007). The depths of Tolstoj and Beethoven are comparable to those of mare-filled lunar basins and martian basins ~100 km in diameter or less. As the surface gravity of Mars is very similar to that of Mercury (3.7 m/s^2), a similar depth-diameter relation for large impact structures might be expected.

Prior to the MESSENGER mission, crater depths on Mercury had been determined solely on the basis of photoclinometry (Pike, 1988) and stereo-derived DEMs (André and Watters, 2006, 2008) of portions of the hemisphere imaged by Mariner 10. Topographic measurements by MLA during MESSENGER's first flyby of Mercury included profiles of several craters, allowing their dimensions to be measured (Zuber et al., 2008) and yielding a ratio d/D of ~1/40. In particular, in cases where the MLA profile crossed near the center of a crater identifiable in Earth-based radar images (Harmon et al., 2007) of the area near the ground track, accurate depth-diameter measurements can be made

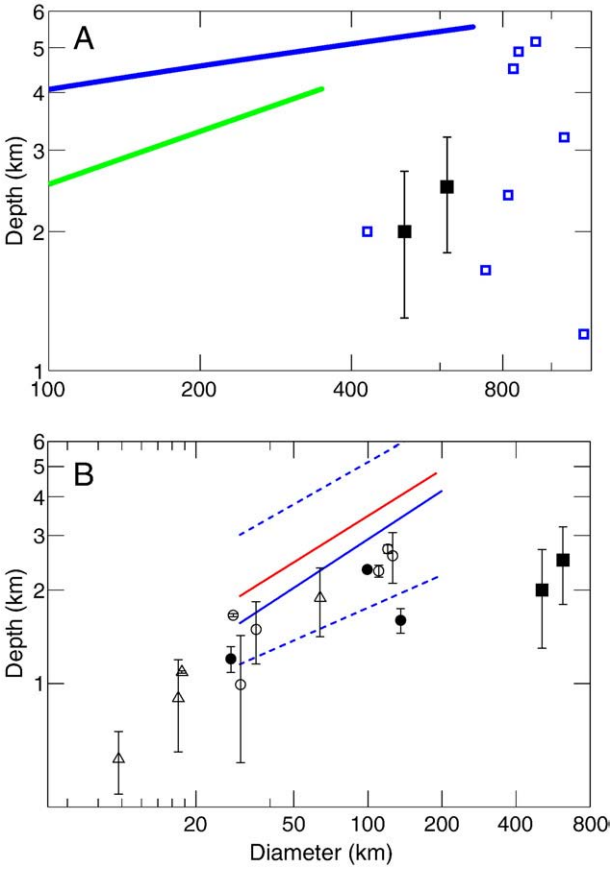

Fig. 1. (A) Depth–diameter relations for lunar basins (blue solid line, Williams and Zuber, 1998) and martian basins (green solid line, Howenstine and Kiefer, 2005) are compared with observations for individual lunar mare basins (open squares, Williams and Zuber, 1998) and for the Tolstoj and Beethoven basins on Mercury (solid squares). (B) Depth–diameter relations for craters and basins on Mercury, from Pike (1988) in red, André and Watters (2007) in blue, MLA observations in circles and triangles, and for Tolstoj and Beethoven (André et al., 2005) in black squares. The dashed blue lines show the approximate range of the depth–diameter data of André and Watters (2007). For the MLA data, open circles represent craters for which the altimeter track crosses near the crater center and the feature is well-aligned with a crater in Earth-based radar images (Harmon et al., 2007); filled circles represent craters well-aligned with a possible crater feature in Earth-based radar images, but ones not centrally transected by the altimeter track; and triangles represent craters poorly aligned with a crater in Earth-based radar images or with a substantially off-center altimeter transect.

for the first time (Fig. 1B). These three databases of dimensions for craters less than 200 km in diameter are in reasonably good agreement. From these datasets, the reported depths of Tolstoj and Beethoven are found to be comparable to those of craters on Mercury ~50–100 km in diameter. They are shallower than the deepest craters measured by Pike (1988) and André and Watters (2006) (d ~4–5 km; see Fig. 2 of André and Watters, 2006) and substantially shallower than even the shallowest 150–200-km-diameter craters measured by these workers. They are similar in depth to the deepest craters measured by MLA, but this coincidence is probably primarily due to the lack of craters greater than 100 km in diameter among the structures so far sampled by MLA.

3. Possible scenarios for shallow basins

Three principal geological explanations for the apparent shallowness of Tolstoj and Beethoven present themselves (see Fig. 2) — volcanic fill, excavation through the crust during basin formation, and viscoelastic relaxation of topographic relief. We assess each of these scenarios in turn, and in Section 4 we evaluate viscoelastic relaxation further through numerical modeling.

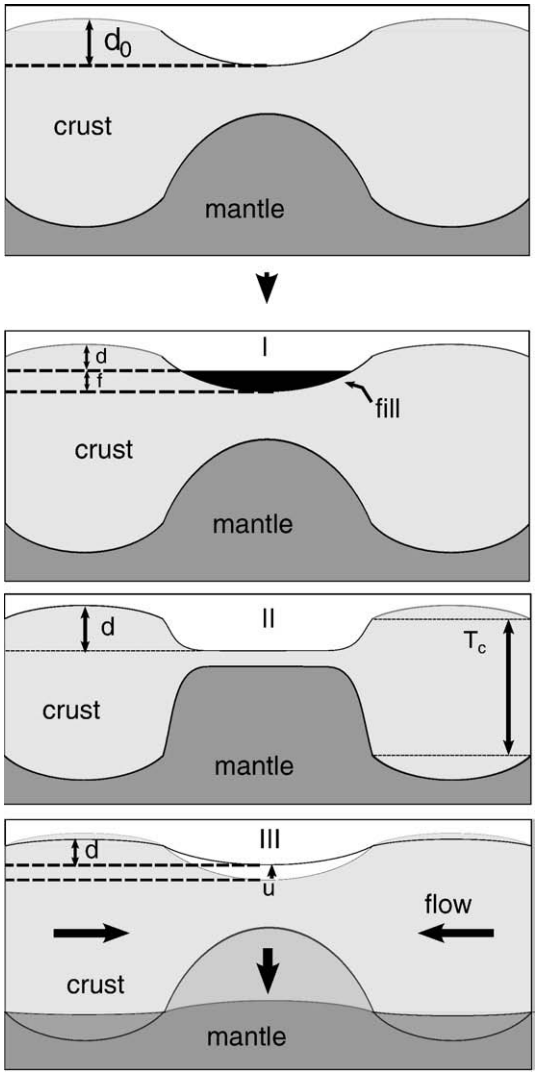

Fig. 2. Depiction of three models to account for the depths of the Beethoven and Tolstoj basins: (I) fill, (II) complete crustal excavation, (III) viscoelastic relaxation. d is the current depth, d_0 is the initial depth (in scenarios I and III), f is the fill thickness, u is the topographic uplift during relaxation, and H_c is the pre-impact crustal thickness.

3.1. Volcanic fill

By analogy with the lunar mare basins, emplacement of volcanic plains in the basin interior could account for the shallow depths (André et al., 2005). In the case where fill accounts entirely for the shoaling and load-induced subsidence is ignored, the current depth d and the initial depth d_0 would be related by

$$d = d_0 - f \tag{1}$$

where f is the thickness of fill. In order to account for the shallowness of the basins, f should be in the approximate range 1–3 km. This thickness of fill should be sufficient to induce flexural subsidence of the basin, yet the floors of Tolstoj and Beethoven do not show the pattern of wrinkle ridges found on the floors of the lunar mare basins, whereas such features are observed within the younger Caloris basin (e.g., Melosh and McKinnon, 1988; Watters et al., 2005; Murchie et al., 2008). Because Mercury has more than double the surface gravitational acceleration of the Moon (1.62 m/s^2) and an almost 50% greater radius (reducing the effect of membrane stresses in supporting loads), the lithosphere of Mercury should experience greater flexure under a given thickness of load than that of the Moon unless it is much more rigid.

Mariner 10 and MESSENGER observations have shown that smooth plains occur within the Caloris, Tolstoj, and Beethoven basins. The interior plains materials in Caloris and Tolstoj are higher in reflectance than and appear to be compositionally distinct from the basin walls and ejects deposits (Robinson et al., 2008). Geological analyses of the plains within Caloris provide strong evidence that they are of volcanic origin (Head et al., 2008; Robinson et al., 2008) and support the inference that wrinkle ridges on the interior plains formed in response to flexural subsidence of the plains (Kennedy et al., 2008; Murchie et al., 2008). By analogy with Caloris, the plains within Tolstoj and Beethoven are also likely to be of volcanic origin. The absence of wrinkle ridges within these basins suggests that if they were filled by plains material to a thickness of 1 km or more, the early lithosphere of Mercury must have been significantly stronger than that which supported the lunar mascons at the time of loading. If lithospheric thickness was not strongly heterogeneous at the time of formation of these basins, then Caloris must have a still greater thickness of interior plains to account for the contractional deformation recorded by its system of wrinkle ridges.

3.2. Crustal excavation

Under the crustal-excavation scenario, the crust was comparatively thin, so large basin-forming impacts exposed mantle material. When an impact excavates the entire crust, the depth is reduced during subsequent crater collapse (whether isostasy is achieved or not) such that the sum of the depth, amplitude of mantle uplift, and melt sheet thickness is equal to the pre-impact crustal thickness. As a result, there will be a maximum basin depth d_{max} that is proportional to the regional crustal thickness. For an isostatic basin, d_{max} is a function of the densities of the crust (ρ_c) and mantle (ρ_m) and the pre-impact crustal thickness (H_c):

$$d_{max} = \left(\frac{\Delta\rho}{\rho_m}\right) H_c \tag{2}$$

where $\Delta\rho = \rho_m - \rho_c$. There is evidence that this scenario may have operated on the Moon, as the largest basins show anomalously shallow apparent excavation depths (Wieczorek and Phillips, 1999; Hikida and Wieczorek, 2007). Where the crustal-excavation scenario holds, the variation of d_{max} across a body permits constraints on large-scale variations in crustal thickness. On the nearside of the Moon

(where the crust is thinnest), for example, many of the large basins are relatively shallow (Williams and Zuber, 1998) and appear to be underlain by little or no crust at present (Hikida and Wieczorek, 2007), while the deepest basins tend to lie in regions of particularly thick crust.

If Beethoven and Tolstoj are shallow because they excavated the entire crust, d_{max} in that area must be ~2–2.5 km or greater, depending on the thickness and compensation state of impact melt and fill. For $d_{max}=2.5$ km, $\Delta\rho=300$–500 kg m^{-3}, and $\rho_m=3200$–3400 kg m^{-3}, Eq. (2) yields $H_c\simeq 15$–30 km. Of course, this relation clearly does not hold for non-isostatic crustal structure, as appears to be the case for most lunar basins (e.g., Neumann et al., 1996; Wieczorek and Phillips, 1999). In non-isostatic situations, d_{max} is likely still proportional to pre-impact crustal thickness, but basins will be shallower than in the isostatic case. For a ratio of crust–mantle-boundary relief to surface relief that is double the isostatic value, $H_c\simeq 30$–55 km. Allowing for post-impact fill would also increase the crustal thickness estimate. On the Moon, large basins that formed in ~40-km-thick crust and appear to have excavated all or almost all of the crust — Humboldtianum, Smythii, and Nectaris (according to the model of Hikida and Wieczorek, 2007) — have depths of 4.2–4.9 km (Williams and Zuber, 1998). If we extrapolate these values to $d_{max}=2.5$ km, we find that $H_c\simeq 20$–25 km. So if Tolstoj and Beethoven did excavate the entire crust, we can expect a pre-impact crustal thickness in the range 15–55 km, depending on the mean densities of the crust and mantle and the final compensation state.

3.3. Viscoelastic relaxation

Viscous flow in the lower crust (Mohit and Phillips, 2006, 2007) has been invoked to explain relaxation of large impact basins on the Moon and Mars. Unless Mercury's crust is substantially thinner than on those bodies, viscous relaxation is also likely to have been important at some point during its history. In such a case, the modified depth of the basin is simply determined by the uplift u experienced during relaxation:

$$d = d_0 - u \tag{3}$$

The uplift will be a strong function of the size of the basin and thickness of the lithosphere at the time of impact (Mohit and Phillips, 2006). We examine this possibility in more detail in the next section.

4. Modeling of viscoelastic relaxation

4.1. Theory

To explore further the relaxation scenario, we employ a spherical, self-gravitating viscoelastic model (Mohit and Phillips, 2006) to determine the conditions necessary for relaxation to take place and the topographic structures that would result. The model solves the equations of conservation of mass and momentum, along with Poisson's equation:

$$v_{i,i} = 0 \tag{4}$$

$$\sigma_{ij,j} + \rho\phi_{,i} + \Delta\rho g\delta_{ir} = 0 \tag{5}$$

$$\phi_{,ii} = 4\pi G\Delta\rho \tag{6}$$

where v is the velocity, σ is the stress tensor, ρ is the density, $\Delta\rho$ is the density anomaly, g is the gravitational acceleration, ϕ is the gravitational potential due to the density anomaly, G is the gravitational constant, subscripts i and j stand in for the three spherical coordinates, δ_{ir} is the Kronecker delta, and the comma denotes partial differentiation with respect to the coordinate that follows. Mercury is treated as a Maxwell viscoelastic body with a layered viscosity structure, such that the stress σ and strain ε are tensors related by

$$\sigma_{ij} + \frac{\eta}{\mu}\dot{\sigma}_{ij} = -P\delta_{ij} + 2\eta\dot{\varepsilon}_{ij} \tag{7}$$

where η is the viscosity, μ is the shear modulus, P is the pressure, and the dot denotes derivative with respect to time.

These equations are reduced to a purely viscous formulation with a Laplace transform (Zhong and Zuber, 2000; Mohit and Phillips, 2006). The dependence of the equations on latitude is eliminated by expanding the initial relief at the surface and crust–mantle interface in spherical harmonics. The equations are then solved by integrating a set of solution vectors from the core–mantle boundary to the surface and finding a linear combination that satisfies the boundary conditions. From the calculus of residues, an inverse Laplace transform is performed, producing a solution of the form

$$h_k(t) = \sum_{l=1}^{M} Rs_l e^{-t/\tau_l} \tag{8}$$

where h_k is the relief at interface k (denoted by s or m for surface or crust–mantle boundary, respectively), M is the number of relaxation modes, Rs_l is the residue and τ_l the relaxation time of the lth mode, and t is time. The number of modes depends on the layering: there is one for each density interface and two for each viscosity interface. See Mohit and Phillips (2006) for details of the solution method.

4.2. Application to Mercury

We consider a suite of simple thermal models similar to those explored by Mohit and Phillips (2006). They consist of a 2-km-thick megaregolith of low thermal conductivity and underlying crust and mantle. The models are parameterized by the crustal thickness H_c and temperature at the base of the crust T_b. For a constant surface temperature, these parameters yield temperature profiles that are relatively insensitive to the unknown thermal conductivity and heat production rate within the crust. We consider a range of crustal thermal conductivities (1.5–3 Wm^{-1} K^{-1}); heat production in the crust is assumed to be chondritic (see Turcotte and Schubert, 1982). For a given T_b, increased crustal thermal conductivity or heat production tends to increase the surface heat flux and thereby the thermal gradient in the megaregolith, thus elevating the brittle–ductile transition and the base of the lithosphere. A low-conductivity layer at the surface can have a strong effect on the temperature profile (cf., Mohit and Phillips, 2006; Parmentier and Zuber 2007); see Fig. 3 for an example. The relevant model parameters are summarized in Table 1.

The rheologies of the crust and mantle are taken to be those of dry diabase (Mackwell et al., 1998) and dry olivine (Karato and Wu, 1993), respectively. The adopted rheology for mantle material is consistent with constraints on convective thermal history models imposed by the cumulative global contraction experienced by Mercury (Hauck et al., 2004). We discuss the effect of the presence of water in the crust or mantle in Section 5. Both rheologies adopted are governed by the following flow law for dislocation creep (see Table 2 for parameters):

$$\dot{\varepsilon} = A\sigma^n e^{\frac{Q}{RT}} \tag{9}$$

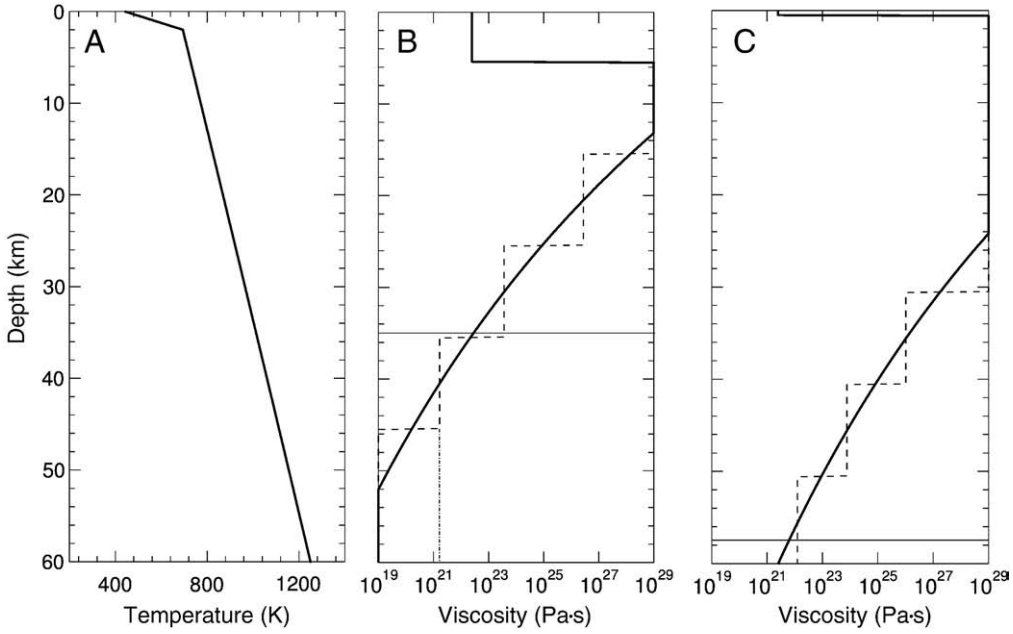

Fig. 3. (A) Temperature profile for $H_c = 60$ km, basal temperature $T_b = 1250$ K. (B) Viscosity profile for $H_c = 60$ km, $T_b = 1250$ K, and a driving stress σ (Eq. (9)) of 50 MPa; the dashed step function shows how the profile is broken into layers, the thin black line indicates the assumed height of initial mantle uplift, and the dash-dot line shows how this uplift determines the thickness of the layer of uniform viscosity at the base of the crust. (C) Viscosity profile for $H_c = 60$ km, $T_b = 1250$ K, $\sigma = 5$ MPa; the dashed line indicates the layered viscosity structure, and the thin black line is the height of mantle uplift at cessation of relaxation.

where ε and σ are suitable invariants of the strain and stress tensors, Q is an activation energy, R is the gas constant, T is absolute temperature, and A and n are constants. The effective viscosity is then

$$\eta_{\text{eff}} = \frac{\sigma}{3\dot{\varepsilon}} \tag{10}$$

As the early thermal evolution and crustal thickness of Mercury are poorly constrained, we consider a wide range of parameters. As initial conditions, we use the topography of the unfilled lunar Mendel–Rydberg basin ($D \sim 600$ km) as a surrogate for the post-impact topography of Beethoven and Tolstoj, and that of Argyre on Mars ($D \sim 1200$ km) as a surrogate for Caloris. In both cases, the topography is expanded to spherical harmonic degree and order 80. As we do not know the crustal structure beneath these basins, we assume that they were initially in local isostatic equilibrium.

For each thermal model, we calculate temperature and viscosity profiles with depth. For ease of computation, we express the latter in terms of discrete layers of uniform viscosity. Because relief on the crust–mantle boundary is represented in the model only as a stress at the interface — analogous to the surface mass approximation used in potential theory (e.g., Wieczorek, 2007) — we treat the depth interval from the shallowest to the deepest levels of the crust–mantle boundary as if it were a uniform layer, and we assign a viscosity appropriate to the steady-state temperature at the top of the layer (Fig. 3B). Such an approach is conservative with respect to degree of relaxation, in the sense that the transient effects of mantle uplift and impact heating on the temperature field are ignored, as are the effects of lower crustal flow more strongly confined to the base of the crust than under the assumptions adopted here. For a full discussion of uncertainties introduced by the neglect of finite-amplitude relief, see Mohit and Phillips (2006). For Beethoven and Tolstoj, we calculate the initial viscosity structure by assuming a driving stress commensurate with ~5 km of relief (50 MPa) and a mantle uplift of 25 km.

We explore a range of mean crustal thickness values between 45 and 140 km, determining in each case the minimum basal temperature (and corresponding basal heat flux) required for relaxation to occur. In addition, we follow the course of the relaxation in order to estimate the remaining relief when relaxation is arrested by the drop in driving stress. As the relief at the crust–mantle boundary relaxes, the crust beneath the floor of the basin thickens, facilitating the process. At the same time, the driving stress decreases, increasing the viscosity. Initially, the former effect dominates; however, once the relief at the crust–mantle boundary drops below about half of its initial value, the decrease in driving stress begins to dominate, slowing relaxation. Once the viscosity at the base of the crust increases above $\sim 10^{22}$ Pa s (see Fig. 3C), relaxation is no longer possible.

Fig. 4 shows examples of relaxation of topographic relief for the Tolstoj and Beethoven case in crust of various thicknesses according to this procedure (summarized in Table 3). Because of the size of the

Table 1
Model parameters.

Parameter	Value	Units
Planetary radius	2440	km
Core radius	1800	km
Gravitational acceleration	3.7	m s^{-2}
Average surface temperature	440	K
Shear modulus	5×10^{10}	Pa
Megaregolith density	2300	kg m^{-3}
Crustal density	2900	kg m^{-3}
Mantle density	3500	kg m^{-3}
Megaregolith thermal conductivity	0.2	W m^{-1} K^{-1}
Crustal thermal conductivity	1.5–3	W m^{-1} K^{-1}
Mantle thermal conductivity	3	W m^{-1} K^{-1}
Crustal heat production	2.3×10^{-11}	W kg^{-1}
Mantle heat production	0	W kg^{-1}
Maximum viscosity	10^{29}	Pa s
Minimum viscosity	10^{19}	Pa s

Table 2
Rheological parameters.

	A (Pa^{-n} s^{-1})	n	Q (kJ mol^{-1})
Columbia diabase	1.2×10^{-26}	4.7	485
Dry olivine	2.4×10^{-16}	3.5	540

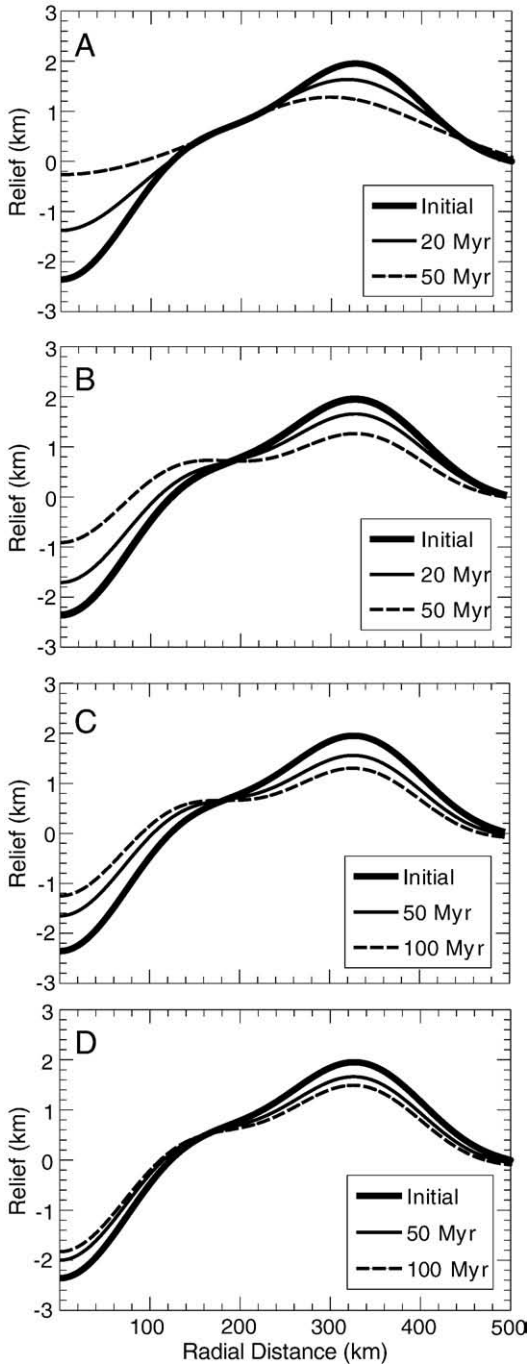

Fig. 4. Relaxation over time of a Beethoven–Tolstoj-sized basin for (A) $H_c = 45$ km, $T_b = 1350$ K; (B) $H_c = 60$ km, $T_b = 1250$ K; (C) $H_c = 80$ km, $T_b = 1200$ K; and (D) $H_c = 100$ km, $T_b = 1150$ K.

structure, the longer wavelengths relax, while the shorter wavelengths are supported by the strength of the lithosphere. As a result, for the relatively cold cases, in which relaxation is possible only when crustal thickness is large (>80 km), a substantial fraction of the initial topography is retained (>2.5 km). If the pre-impact crust is relatively thin (e.g., the 45-km case), high temperatures in the lower crust are necessary in order to permit relaxation, and less topography remains (<1 km) because of the thin lithosphere. The uncertainty in the depths of the two basins requires that we consider a range of 1–3 km of remaining topography as plausible; this range results in a minimum crustal thickness required for relaxation of 45–100 km. As any crust

Table 3
Results.

H_c (km)	T_b (K)	Heat flux (W m^{-2})	Relief (km)
45	1350	20–40	1
60	1250	15–30	2
80	1200	11–23	2.5
100	1100	9–18	3

T_b is the minimum basal temperature required to permit flow in crust with background thickness H_c, and "relief" is the post-relaxation relief.

thicker than 100 km suffices (given appropriate thermal conditions), we do not show results for thicker crust than this limit.

For Caloris, we consider two cases: one in which the initial relief on the crust–mantle boundary is ~25 km — comparable to that of Mendel–Rydberg on the Moon or Argyre basin on Mars — and one in which the initial relief is ~35 km, comparable to that of the martian Isidis basin (Neumann et al., 2004); for the latter case, the surface topography is correspondingly increased. An example of each is shown in Fig. 5. In the former case, relaxation proceeds more slowly than for Tolstoj and Beethoven (because of the long-wavelength flow required), but relaxation does occur on a timescale of ~10^8 years for a comparable viscosity structure. In the high-relief case, on the other hand, greater temperatures are required in the lower crust for relaxation to proceed. For $H_c = 80$ km, T_b need only be increased to 1300 K. For $H_c \leq 60$ km, shrinking the crustal channel to less than ~25 km thickness, however, the critical $T_b \geq 1400$ K and increases rapidly as crustal thickness decreases. In both cases, little surface topography is retained, as there is insufficient power at wavelengths sufficiently short to be supported by the lithosphere.

5. Discussion

The topographic information derived from Mariner 10 images suggests that the two major basins Beethoven and Tolstoj are shallower

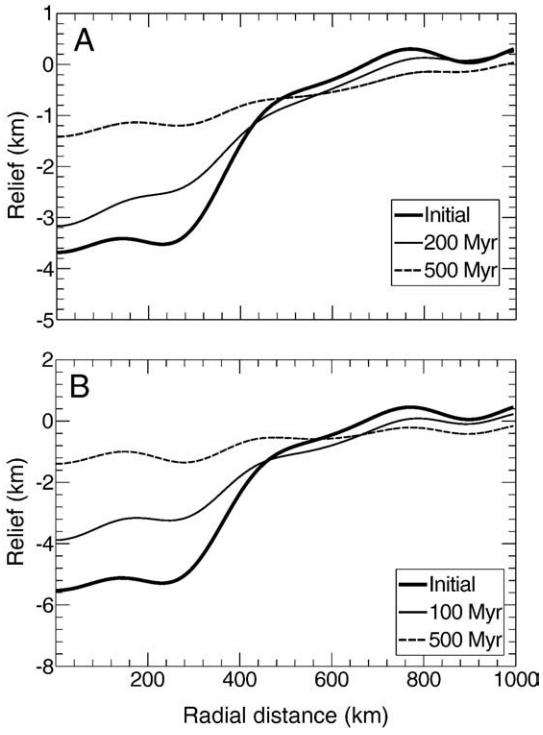

Fig. 5. Relaxation over time of a Caloris-sized basin for (A) $H_c = 60$ km, $T_b = 1250$ K, for an initial mantle uplift of 25 km; (B) $H_c = 80$ km, $T_b = 1300$ K, for an initial mantle uplift of 35 km.

than would be expected for their size, the result of some combination of volcanic fill, excavation of thin crust, and viscoelastic relaxation. The idea that emplacement of smooth plains material accounts for the shallow depths has been explored by other workers (André et al., 2005). Tolstoj and Beethoven show similar depths to lunar mare basins, and the smooth plains deposits in these basins are extensive. However, little or no tectonic evidence of flexure in response to the load (e.g., concentric wrinkle ridges and graben) is observed, requiring more rigid lithosphere than that which faulted in response to lunar mascon loading.

Our analysis has focused on the relaxation scenario, with the objective of determining: (1) whether the occurrence of viscoelastic relaxation on Mercury is plausible, (2) under what conditions it would be likely to have occurred, and (3) how to distinguish among scenarios with observations to be made by MESSENGER. The results presented here show that the proposal that Beethoven and Tolstoj have relaxed is plausible. However, the model of Watters et al. (2005) shows that viscous relaxation of the Caloris basin may have produced sufficient extensional stresses to result in extensional faulting within the basin. Similarly, the relaxation of Beethoven or Tolstoj would be expected to have produced extensional stress, albeit weaker and over shorter length scales. So, the lack of extensional faulting suggests that either: (1) no relaxation took place, (2) the amplitude of extensional stress in the lithosphere was insufficient to produce faulting, or (3) extensional faults were formed but were later buried by interior smooth plains.

The modeling results show that thick crust (100 km) and low heat flow (10–20 mW m^{-2}) would permit up to 3 km of relief to be retained for Beethoven and Tolstoj. A crustal thickness less than 60 km, in contrast, would require sufficiently high temperatures in the crust for relaxation to proceed that less than 2 km of relief would be retained. These results must be applied to Mercury with caution because of our limited state of knowledge regarding the planet. Current estimates for the depths of Tolstoj and Beethoven are in the range 1–3 km, requiring a minimum crustal thickness of 45–100 km in order for relaxation to occur. Uncertainties in the density, heat production, and thermal conductivity of crust and mantle, while great, have little effect on these lower bounds. For a given (T_b, H_c) parameter set, increased crustal heat production or thermal conductivity would tend to raise slightly the depth to the brittle–ductile transition and the base of the lithosphere, potentially facilitating relaxation. However, unless heat production approaches that in KREEP-rich lunar rocks, the effect should be negligible (cf. Mohit and Phillips, 2006).

The density difference between crust and mantle, on the other hand, could have a strong influence on relaxation, as it affects the amplitude of mantle uplift. That assumed here is consistent with what is known of the densities of lunar and martian materials. The density contrast on Mercury may be lower, however, because of the lesser iron abundance in Mercury's mantle and crustal materials. A lower density contrast would tend to increase the amplitude of mantle uplift relative to the basin depth, resulting in a thinner crust beneath the basin floors and increasing the crustal thickness bounds discussed here. If the deformation of the crust and mantle of Mercury is governed by flow laws appropriate to material containing even small quantities of water, then thinner crust might be permissible. Under these circumstances, the scenarios with thicker crust would become less likely, as unrealistically low values of heat flow would be required.

The case of Caloris is more uncertain, as its depth is ill-constrained. The only measurement available gives a depth of 9 ± 3 km, suggesting that it has not relaxed and is one of the deepest basins in the Solar System. However, the presence of extensional tectonic features within the basin is likely an indication of past relaxation (Watters et al., 2005). Modeling of Caloris shows that relaxation is inhibited if the crustal thickness beneath the basin floor is less than ~25 km. Thus, it is possible for Beethoven and Tolstoj to have relaxed while Caloris did not if the crust is thinner than a critical value. It is not, on the other hand, possible for Caloris to have relaxed but not Beethoven and Tolstoj, unless there were large lateral variations in crustal thickness or heat flux on Mercury at the time of basin formation. We note that if viscous relaxation played a role in the evolution of all three basins, then Beethoven and Tolstoj may have retained more topography than Caloris, depending on thermal conditions and crustal thickness at the three sites. Clearly, an accurate depth determination for Caloris is critical to an evaluation of the relaxation hypothesis.

The crustal-excavation scenario is not entirely consistent with the available data sets, but the uncertainty in current data prevents it from being ruled out. The first problem is that there are craters in existing Mercury data sets that are deeper than Beethoven and Tolstoj, implying that the depths of these two basins do not represent a global maximum. Depending on the locations of the deeper craters, this result may be explained by invoking lateral variations in crustal thickness. However, if Caloris is as deep as the photoclinometric estimate suggests, then the regional crustal thickness would have to vary by a factor of at least 3. If the 9-km depth of Caloris is validated, the crustal-excavation scenario can be rejected and a lower limit placed on the pre-impact crustal thickness. On the other hand, if future measurements of the depths and gravity anomalies of northern basins are consistent with this scenario, then the spatial distribution of crater and basin depths could be used to constrain long-wavelength variations in crustal thickness. The depth estimates of Beethoven and Tolstoj from stereogrammetry point to a crustal thickness of 15–55 km in that area. Given the uncertainty in these estimates, a range of 10–70 km may be possible.

The three scenarios for shallow basin depths have different implications for the early history of Mercury. In particular, either the viscoelastic-relaxation or crustal-excavation scenario would place constraints on the crustal thickness, independent of uncertainties in the thermal conductivity and surface heat flux. The primary uncertainties in the relaxation scenario pertain to the rheology of the crust, and those in the crustal-excavation scenario are the densities of the crust and mantle. Spectral measurements of the composition of the crust should aid in improving current estimates of several of these parameters.

Validation of the volcanic-fill scenario would point to an early thick lithosphere on Mercury. It would say little about the crustal thickness directly, although a lower bound could be established using the arguments relating to thin crust. The greatest contribution to be made by these models is to help distinguish among the hypotheses for Mercury's formation and bulk composition. A constraint on crustal thickness would be an important step in that direction, as the three principal hypotheses make different predictions regarding crustal composition and, secondarily, thickness. Both the vaporization and impact stripping hypotheses involve removal of much if not all of the early crust. Thus, they would be difficult to reconcile with the relaxation scenario. Conversely, the crustal-excavation scenario would be supportive of models in which the early crust had been removed.

6. Conclusions and future measurements

We have examined three scenarios to explain the shallow depths of Beethoven and Tolstoj basins (André et al., 2005) on Mercury: volcanic fill, excavation of thin crust, and viscoelastic relaxation. In addition we have evaluated the implications of each scenario for explaining the large depth proposed for the Caloris basin (Hapke et al., 1975). On the basis of currently available data, all three scenarios remain possible. However, current constraints are poor and all three explanations face challenges in accounting for both the shallow depths of Beethoven and Tolstoj and the greater depth of Caloris. We consider the depth estimates for Beethoven and Tolstoj to be more reliable than that for Caloris, but all of the published estimates are likely affected by long-wavelength biases.

The second and third MESSENGER flybys will enhance existing depth–diameter data sets and — perhaps most importantly — enable a

Table 4
Possible MESSENGER observations and their implications.

Observation	Implication
Basins show a variety of depths and strong positive gravity anomalies.	The basins have been filled, requiring a strong lithosphere.
Almost all basins are similar in depth to, or shallower than, Tolstoj and Beethoven and show negative gravity anomalies.	Viscous relaxation has likely occurred (Mohit and Phillips, 2006).
Basins show depths comparable to Tolstoj and Beethoven (or vary on a regional basis) and isostatic gravity anomalies.	Crustal thickness is likely controlling the depths of the basins.
Caloris is 9 km deep; other basins display shallow depths and negative gravity anomalies.	The crust beneath the floor of Caloris is probably <15–20 km thick, providing an upper bound on the thickness in that area.
Caloris is shallow but retains a sharp topographic structure.	Complete crustal excavation is likely, placing a lower bound on the thickness in that area.
Caloris shows shallow topographic slopes	The basin has at least partially relaxed; detailed modeling should yield constraints on the post-impact thermal structure and crustal thickness.

comparison of stereo elevation models with laser altimetric measurements. This comparison will provide the information necessary to evaluate long-wavelength biases in existing stereo models. The second flyby occurred on October 6, 2008, and the third will take place on September 29, 2009. Once MESSENGER enters orbit about Mercury in March 2011, MLA will map almost the entire northern hemisphere, and a gravity model will be produced with an average resolution of ~400 km in the northern hemisphere (Solomon et al., 2001), providing additional information on the compensation states of major basins. The improved imaging and topography data sets expected during the orbital phase of the mission will also aid in clarifying the tectonic histories of impact basins. In particular, these data sets should provide some insight into the thickness of volcanic fill in at least the northern basins and may reveal evidence of tectonic deformation partially buried by the later emplacement of basin-interior plains.

Although the topography and gravity maps will not extend southward to Beethoven and Tolstoj specifically, several basins of comparable size have been identified in the northern hemisphere (Pike and Spudis, 1987). In addition, the depth and gravity signature of Caloris will be accurately measured. These measurements will allow further testing of the scenarios presented here and their relative roles in basin evolution on Mercury. Table 4 lists possible future gravity and topography observations and their implications.

The observations and models discussed in this paper suggest that the evolution of major impact basins on Mercury has followed a different path from those of lunar and martian basins. The data sets to be acquired during the remainder of the MESSENGER mission (and future missions) should allow us to reconstruct some of the conditions prevailing early in Mercury's history and help distinguish among hypotheses for the planet's formation.

Acknowledgements

CLJ and PSM were supported by the NASA Planetary Geology and Geophysics and MESSENGER Participating Scientist programs under grants NNG05GK34G and NNX07AR73G. CLJ acknowledges the Kavli Institute for Theoretical Physics (National Science Foundation grant PHY05-51164) and the Cooperative Institute for Deep Earth Research (NSF grant EAR-0434151) for support and interactions during the preparation of this manuscript. The MESSENGER project is supported by the NASA Discovery Program under contracts NASW-00002 to the Carnegie Institution of Washington and NAS5-97271 to the Johns Hopkins University Applied Physics Laboratory. We also thank Jay Melosh and an anonymous reviewer for thorough and constructive reviews.

References

Anderson, J.D., Jurgens, R.F., Lau, E.L., Slade III, M.A., Schubert, G., 1996. Shape and orientation of Mercury from radar ranging data. Icarus 29, 690–697.
André, S.L., Watters, T.R., 2006. Depth to diameter measurements of mercurian mature complex craters. Lunar Planet. Sci. 37, abstract 2054.
André, S.L., Watters, T.R., 2007. Mercury stereo topography: construction of regional topographic maps derived from Mariner 10 images. Lunar Planet. Sci. 38, abstract 2155.
André, S.L., Watters, T.R., 2008. Depth to diameter studies of mercurian mature complex craters using Mariner 10 stereo topography. Lunar Planet. Sci. 39, abstract 2066.
André, S.L., Watters, T.R., Robinson, M.S., 2005. The long wavelength topography of Beethoven and Tolstoj basins, Mercury. Geophys. Res. Lett. 32, L21202. doi:10.1029/2005GL023627.
Benz, W., Anic, A., Horner, J., Whitby, J.A., 2007. The origin of Mercury. Space Sci. Rev. 132, 189–202.
Breuer, D., Hauck II, S.A., Buske, M., Pauer, M., Spohn, T., 2007. Interior evolution of Mercury. Space Sci. Rev. 132, 229–260.
Hapke, B., Danielson Jr., G.E., Klaasen, K., Wilson, L., 1975. Photometric observations of Mercury from Mariner 10. J. Geophys. Res. 80, 2431–2443.
Harmon, J.K., Slade, M.A., Butler, B.J., Head, J.W., Rice, M.S., Campbell, D.B., 2007. Mercury: radar images of the equatorial and midlatitude zones. Icarus 187, 374–405.
Hauck II, S.A., Dombard, A.J., Phillips, R.J., Solomon, S.C., 2004. Internal and tectonic evolution of Mercury. Earth Planet. Sci. Lett. 222, 713–728.
Head III, J.W., Murchie, S.L., Prockter, L.M., Robinson, M.S., Solomon, S.C., Strom, R.G., Chapman, C.R., Watters, T.R., McClintock, W.E., Blewett, D.T., Gillis-Davis, J.J., 2008. Volcanism on Mercury: evidence from the first MESSENGER flyby. Science 321, 69–72.
Hikida, H., Wieczorek, M.A., 2007. Crustal thickness of the Moon: new constraints from gravity inversions using polyhedral shape models. Icarus 192, 150–166.
Howenstine, J.B., Kiefer, W.S., 2005. Morphometry of large martian impact craters. Lunar Planet. Sci. 36 abstract, 1742.
Karato, S.I., Wu, P., 1993. Rheology of the upper mantle: a synthesis. Science 260, 771–778.
Kennedy, P.J., Freed, A.M., Solomon, S.C., 2008. Mechanisms of faulting in and around Caloris basin, Mercury. J. Geophys. Res. 113, E08004. doi:10.1029/2007JE002992.
Mackwell, S.J., Zimmerman, M.E., Kohlstedt, D.L., 1998. High-temperature deformation of dry diabase with application to tectonics on Venus. J. Geophys. Res. 103, 975–984.
Melosh, H.J., McKinnon, W.B., 1988. The tectonics of Mercury. In: Vilas, F., Chapman, C.R., Mathews, M.S. (Eds.), Mercury. University of Arizona Press, Tucson, Ariz., pp. 374–400.
Mohit, P.S., Phillips, R.J., 2006. Viscoelastic evolution of lunar multiring basins. J. Geophys. Res. 111, E12001. doi:10.1029/2005JE002654.
Mohit, P.S., Phillips, R.J., 2007. Viscous relaxation on early Mars: a study of ancient impact basins. Geophys. Res. Lett. 34, L21204. doi:10.1029/2007GL031252.
Murchie, S.L., Watters, T.R., Robinson, M.S., Head, J.W., Strom, R.G., Chapman, C.R., Solomon, S.C., McClintock, W.E., Prockter, L.M., Domingue, D.L., Blewett, D.T., 2008. Geology of the Caloris basin, Mercury: a view from MESSENGER. Science 321, 73–76.
Neumann, G.A., Zuber, M.T., Smith, D.E., Lemoine, F.G., 1996. The lunar crust: global structure and signature of major basins. J. Geophys. Res. 101, 16841–16864.
Neumann, G.A., Zuber, M.T., Wieczorek, M.A., McGovern, P.J., Lemoine, F.G., Smith, D.E., 2004. Crustal structure of Mars from gravity and topography. J. Geophys. Res. 109, E08002. doi:10.1029/2004JE002262.
Nimmo, F., 2002. Constraining the crustal thickness on Mercury from viscous topographic relaxation. Geophys. Res. Lett. 29, 1063. doi:10.1029/2001GL013883.
Parmentier, E.M., Zuber, M.T., 2007. Early evolution of Mars with mantle compositional stratification or hydrothermal crustal cooling. J. Geophys. Res. 112, E02007. doi:10.1029/2005JE002626.
Pike, R.J., 1988. Geomorphology of impact craters on Mercury. In: Vilas, F., Chapman, C.R., Mathews, M.S. (Eds.), Mercury. University of Arizona Press, Tucson, Ariz., pp. 165–273.
Pike, R.J., Spudis, P.D., 1987. Basin-ring spacing on the Moon, Mercury, and Mars. Earth Moon Planets 39, 129–194.
Robinson, M.S., Murchie, S.L., Blewett, D.T., Domingue, D.L., Watters, T.R., Hawkins III, S.E., Head III, J.W., Holsclaw, G.M., McClintock, W.E., McCoy, T.J., McNutt Jr., R.L., Prockter, L.M., Solomon, S.C., 2008. Reflectance and color variations on Mercury: regolith processes and compositional heterogeneity. Science 321, 66–69.
Schaber, G.G., McCauley, J.F., 1980. Geologic map of the Tolstoj quadrangle of Mercury. Map I-1199 (H-8), Misc. Investigations Ser., U.S. Geological Survey, Denver, Colo.
Schenk, P.M., Bussey, D.B.J., 2004. Galileo stereo topography of the lunar north polar region. Geophys. Res. Lett. 31, L23701. doi:10.1029/2004GL021197.
Solomon, S.C., 2003. Mercury: the enigmatic innermost planet. Earth Planet. Sci. Lett. 216, 441–455.
Solomon, S.C., McNutt Jr., R.L., Gold, R.E., Acuña, M.H., Baker, D.N., Boynton, W.V., Chapman, C.R., Cheng, A.F., Gloeckler, G., Head III, J.W., Krimigis, S.M., McClintock, W.E., Murchie, S.L., Peale, S.J., Phillips, R.J., Robinson, M.S., Slavin, J.A., Smith, D.E., Strom, R.G., Trombka, J.I., Zuber, M.T., 2001. The MESSENGER mission to Mercury: scientific objectives and implementation. Planet. Space Sci. 49, 1445–1465.
Spudis, P.D., Prosser, J.G., 1984. Geologic map of the Michelangelo quadrangle of Mercury. Map I-1659 (H-12), Misc. Investigations Ser, U.S. Geological Survey, Denver, Colo.
Spudis, P.D., Guest, J.E., 1988. Stratigraphy and geologic history of Mercury. In: Vilas, F., Chapman, C.R., Mathews, M.S. (Eds.), Mercury. University of Arizona Press, Tucson, Ariz., pp. 118–164.
Turcotte, D.L., Schubert, G., 1982. Geodynamics: Applications of Continuum Physics to Geological Problems. John Wiley and Sons, New York. 450 pp.
Watters, T.R., Schultz, R.A., Robinson, M.S., Cook, A.C., 2002. The mechanical and thermal structure of Mercury's early lithosphere. Geophys. Res. Lett. 29, 1542. doi:10.1029/2001GL014308.

Watters, T.R., Nimmo, F., Robinson, M.S., 2005. Extensional troughs in the Caloris basin on Mercury: evidence of lateral crustal flow. Geology 3, 669–672.
Wieczorek, M.A., 1988. Gravity and topography of the terrestrial planets. In: Schubert, G. (Ed.), Treatise on Geophysics, vol. 10. Elsevier, New York, pp. 165–206.
Wieczorek, M.A., Phillips, R.J., 1999. Lunar multiring basins and the cratering process. Icarus 139, 246–259.
Wieczorek, M.A., Zuber, M.T., 2004. Thickness of the martian crust: improved constraints from geoid-to-topography ratios. J. Geophys. Res. 109, E01009. doi:10.1029/2003JE002153.
Wieczorek, M.A., Jolliff, B.L., Khan, A., Pritchard, M.E., Weiss, B.P., Williams, J.G., Hood, L.L., Righter, K., Neal, C.R., Shearer, C.K., McCallum, I.S., Tompkins, S., Hawke, B.R., Peterson, C., Gillis, J.J., Bussey, B., 2006. The constitution and structure of the lunar interior. Rev. Min. Geochem. 60, 221–364.
Williams, K.K., Zuber, M.T., 1998. Measurement and analysis of lunar basin depths from Clementine altimetry. Icarus 131, 107–122.
Zhong, S., Zuber, M.T., 2000. Long-wavelength topographic relaxation for self-gravitating planets and implications for the time-dependent compensation of surface topography. J. Geophys. Res. 105, 4153–4164.
Zuber, M.T., Smith, D.E., Solomon, S.C., Phillips, R.J., Peale, S.J., Head III, J.W., Hauck II, S.A., McNutt Jr., R.L., Oberst, J., Neumann, G.A., Lemoine, F.G., Sun, X., Barnouin-Jha, O., Harmon, J.K., 2008. Laser altimeter observations from MESSENGER's first Mercury flyby. Science 132, 77–79.